# Topological Symmetry of High Rank and Genus Clusters

Modjtaba Ghorbani[a*], Atena Pîrvan-Moldovan,[b] Fatemeh Koorepazan-Moftakhar[c]
[a]Department of Mathematics, Faculty of Science, Shahid Rajaee Teacher Training University, Tehran, 16785-136, I. R. Iran
[b]Department of Chemistry, Faculty of Chemistry and Chemical Engineering, "Babes-Bolyai University,
Arany Janos Str. 11, 400028, Cluj, Romania. E-mail: diudea@gmail.com.
[c]Faculty of Mathematical Sciences, University of Kashan, Kashan 87317, I. R. Iran

***Abstract**: Matter is organized according to its constituents **s**ymmetry. Topological symmetry refers to the maximum possible symmetry achievable by a molecular structure; it is invariant to translations and rotations. Topological symmetry may be found either by permutations within the adjacency matrix of its associate graph or by calculating values of some topological indices. This paper presents the equivalence classes of substructures of some high rank and high genus clusters, with icosahedral and octahedral symmetry, designed by operations on maps and solved by using two topological indices: ring signature index RSI and centrality index C, computed both on isolated structures and selections "immersed" on the bulk networks. Design of multi-shell clusters was performed at TOPO GROUP CLUJ by the original CVNET and Nano Studio software programs.*

***Keywords**: topological symmetry; higher rank cluster; centrality; ring signature.*

## 1. INTRODUCTION

Molecular topology reveals a symmetry different from the geometrical symmetry, namely the constitutional or topological symmetry, which is defined in terms of connectivity; its main goal is to find the equivalence relationship existing among the substructures of a molecular graph: vertices/atoms, edges/bonds, faces, etc. (Ashrafi et al. 2013; Diudea and Nagy 2007, 2013).
Let $X = \{1,2,\ldots,n\}$; a permutation group on $X$ is a group $\Gamma$ whose elements are permutations of $X$, *e.g.* bijective functions from $X$ to $X$ and whose group operation is the composition of permutations in $\Gamma$. The group of all permutations of $X$ is the symmetric group of $X$ denoted by $S_X$ or $S_n$, where $X$ is finite and $n = |X|$. By this notation, a finite permutation group is a subgroup of the symmetric group $S_n$.
An automorphism of the graph $G$= (V, $E$) is a bijection $\sigma$ on V which preserves the edge set $E$, namely $e = uv$ is an edge if and only if $\sigma(e) = \sigma(u)\sigma(v)$ is an edge of $E$ . Here, the image of vertex $u$ is denoted by $\sigma(u)$. The set of all automorphisms of a graph $G$, with the permutation composition operation, is a permutation group on V($G$), denoted by Aut($G$). Note that, in general, the symmetry group of a graph is a subgroup of its automorphism group. For example, in a fullerene graph, both of them are equal; in many other molecular graphs, such as dendrimers, the symmetry group is a proper subgroup of its automorphism groups.
**Example 1.** Consider the molecular graph $H_2O$ of water molecule as depicted in Figure 1; the function

$$f = \begin{pmatrix} 1 & 2 & 3 \\ 2 & 1 & 3 \end{pmatrix} = (1,2)$$

is a symmetry element of this graph. Since a group is closed under the group operation (1,2)(1,2) = $id$, it is an automorphism of molecular graph of $H_2O$. An identity permutation of the graph vertices is denoted by (). Hence, the automorphism group of this graph is represented as {(),(1,2)}. This group is isomorphic with the cyclic group $C_2$.

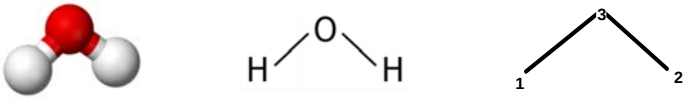


**Figure 1:** The graph of water molecule.

The adjacency matrix A($G$) of graph $G$ with the vertex set V($G$)= $\{v_1, v_2, \ldots, v_n\}$ is the $n\times n$ symmetric matrix $[a_{ij}]$ such that $a_{ij} = 1$ if $v_i$ and $v_j$ are adjacent and 0, otherwise. Suppose $\sigma$ is a permutation on $n$ atoms of the

molecular graph $G$ under consideration and $P_\sigma$ is the permutation matrix of $G$. It is well-known that $P_\sigma P_\tau = P_{\sigma\tau}$, for any two permutations $\sigma$ and $\tau$ on $n$ vertices of $G$ and so the set of all $n\times n$ permutation matrices is a group isomorphic to the symmetric group $S_n$ on $n$ symbols. To compute the automorphism of a graph it is sufficient to solve the matrix equation

$$P^t \mathrm{A} P = \mathrm{A}, \qquad (1)$$

where A is the adjacency matrix of $G$ and $P$ varies on the set of all permutation matrices with the same dimension as A. In other words, if $\sigma$ is a permutation of vertices of $G$, then $\sigma \in Aut(G)$ if and only if $P_\sigma^t A P_\sigma = A$.

**Example 2.** Consider the (labeled) graph of naphthalene (Figure 2, left). Let $\lambda$=(1,9)(2,10)(3,7)(4,8) and $\omega$=(1,2)(3,4)(5,6)(7,8)(9,10) be two permutations of vertices of naphthalene molecular graph. We show that the permutation matrix of both of them satisfies Eq. (1). The adjacency matrix of the naphthalene graph and the permutation matrix with respect to $\lambda$ are as follows:

$$A = \begin{bmatrix} 0&1&1&0&0&0&0&0&0&0\\ 1&0&0&1&0&0&0&0&0&0\\ 1&0&0&0&1&0&0&0&0&0\\ 0&1&0&0&0&1&0&0&0&0\\ 0&0&1&0&0&1&1&0&0&0\\ 0&0&0&1&1&0&0&1&0&0\\ 0&0&0&0&1&0&0&0&1&0\\ 0&0&0&0&0&1&0&0&0&1\\ 0&0&0&0&0&0&1&0&0&1\\ 0&0&0&0&0&0&0&1&1&0 \end{bmatrix}. \qquad P_\lambda = \begin{bmatrix} 0&0&0&0&0&0&0&1&1&0\\ 0&0&0&0&0&0&0&1&1&0\\ 0&0&0&0&1&0&0&0&1&0\\ 0&0&0&0&0&1&0&0&0&1\\ 0&0&1&0&0&1&1&0&0&0\\ 0&0&0&1&1&0&0&1&0&0\\ 1&0&0&0&1&0&0&0&0&0\\ 0&1&0&0&0&1&0&0&0&0\\ 0&1&1&0&0&0&0&0&0&0\\ 1&0&0&1&0&0&0&0&0&0 \end{bmatrix}.$$

It is not difficult to see that $P_\lambda$ satisfies Eq.(1) and hence $\lambda$ is an automorphism element. Similarly, we can prove that $\omega$ is an automorphism and thus the permutation of its automorphism group is as follows:
{(), (1,9)(2,10)(3,7)(4,8), (1,2)(3,4)(5,6)(7,8)(9,10), (1,10)(2,9),(3,8),(4,7),(5,6)}.

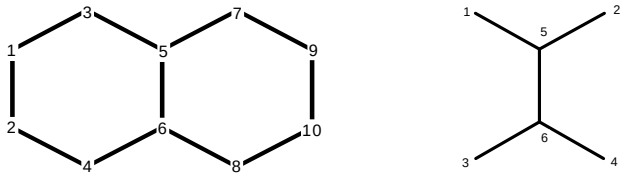


**Figure 2.**The molecular graphs of naphthalene (left) and 2,3 Dimethyl-butane (right)

Suppose $\Gamma_1$ and $\Gamma_2$ are two groups and $\Gamma_2$ acts on the set $\Omega$. The wreath product of $\Gamma_1 \wr \Gamma_2$ is defined as the set of all order pairs $(f;\lambda)$ where $\lambda \in \Gamma_2$ and $f$: $\Omega \rightarrow \Gamma_1$ is a function, such that $(f_1; \lambda_1)(f_2; \lambda_2)=(g; \lambda_1\lambda_2)$ where $g(i) = f_1(i) f_2(i^{\lambda_1})$. Observe that if $\Omega$, $\Gamma_1$ and $\Gamma_2$ are finite then $|\Gamma_1 \wr \Gamma_1| = |\Gamma_1|^{|\Omega|}|\Gamma_2|$. Finally, consider the graph G depicted in Figure 2 (right). The symmetry group of G is Sym(G) = {(),(1,2)(3,4),(1,3)(2,4)(5,6),(1,4),((2,3)(5,6)}; it is isomorphic with the non-cyclic abelian group $C_2 \times C_2$ of order 4 while the permutation (1,2) is a graph automorphism of G. On the other hand, it can be shown that Aut(G) = $C_2 \wr C_2$, which is of order 8. All elements of Aut($G$) are as follows: {(),(1,2)(3,4),(1,3)(2,4)(5,6), (1,4)(2,3)(5,6), (1,2),(3,4), (1,3,2,4)(5,6), (1,4,2,3)(5,6)}. Thus, $Sym(G) \subset Aut(G)$.

In the theory of groups action (Hungerford, 1974), the group $G$ is said to act on a set X if there is a function $\phi$ such that $\phi$: G×X⟶X and for any element x∈X, there exists the relation $\phi(g,\phi(h,x))=\phi(gh,x)$, for all g,h∈G, with $\phi(e,x)=x$, $e$ being the identity element of $G$. The mapping $\phi$ is called a group action while the set $\{\phi(gx) \mid g\in G\}$ or $x^G$ (in brief) is called the orbit of $x$. Hence, $x^G = \{x^g: g\in G\}$.

Suppose that $G$ acts on X, for each x∈X, the stabilizer of $x$ denoted by $G_x$ is a subgroup of $G$ and can be defined as follows: $G_x = \{ g\in G: x^g = x\}$.

**Orbit Stabilizer Theorem.** Let $G$ be a group acting on the set X. Then, for every element $x\in X$, the size of orbit $x^G$ is $|x^G| = [G: G_x]$. Let also $G$ be a group acting on a set X; for every element $g\in G$, denote by fix($g$) the set of elements in X that are fixed by $g$ namely, $\mathrm{fix}_X(g) = \{ x\in X, x^g = x\}$.

**Cauchy-Frobenius Lemma**. The number of orbits of X under the action of $G$ is:

$$t = \frac{1}{|G|}\sum_{g\in G} |\, fix(g)\,|. \qquad (2)$$

Consider now the graph $G$ depicted in Figure 3. By the above notation, we have:
$1^G = 2^G = 3^G = 4^G = \{1,2,3,4\}$ ; $5^G = 6^G = \{5,6\}$.
On the other hand, |fix()| = 6, |fix((1,2)(3,4))| = 2, |fix((1,2))| = |fix((3,4))| = 4, |fix((1,3)(2,4)(5,6))| = |fix((1,4)(2,3)(5,6))| = |fix((1,3,2,4)(5,6))| = |fix((1,4,2,3)(5,6))| = 0.
Hence, by using the above (eq. 2), we have:
Number of orbits (equivalence classes) = (6 + 2 + 4 + 4 + 0 + 0 +0 + 0)/8 = 2.
Namely, there are 2 orbits of size: 2, 4.

**Example 3.** Consider the graph depicted in Figure 3. By using GAP program (GAP, 2014), one can see that Aut($G$) = $C_2 \times S_4$ (in Chemistry: $C_2 \times T_d$) of order $2 \times 24 = 48$. There are 11 orbits, of size: 8,8,6,6,24,24,24,24,24,6,6 respectively.

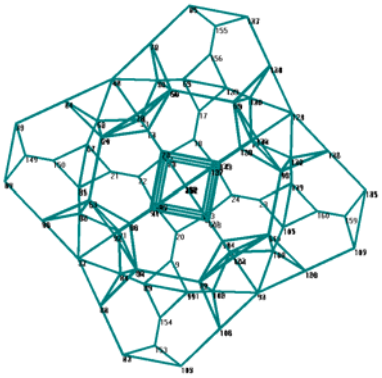

**Figure 3.** A (labeled) graph on160 vertices.

Suppose $v_1,v_2,...,v_m$ are $m$ disjoint automorphic partitions of the set of vertices V(H), then: $V = V_{v1} \cup V_{v2} \cup ... \cup V_{vm}$ and $V_{v_i} \cap V_{v_j} = \varnothing$. An invariant assigning the values $In_i$ and $In_i$ to vertices i, j∈V will provide invariant classes of equivalence that may differ from the automorphism classes/orbits, since no vertex invariant is known so far to always discriminate two non-equivalent vertices in any graph. The classes of vertices may be ordered according to some rules.

An embedding is a representation of a graph on a surface $S$ such that no edge-crossing occurs (Harary, 1969). A polyhedral graph, embedded in an orientable surface $S$ obeys the Euler's theorem (Euler, 1752-3):

$$v - e + f = \chi(S) = 2(1-g) \qquad (3)$$

where $\chi(S)$ is the Euler characteristic and g the genus (i.e., the number of consisting simple tori). Positive/negative χ-values indicate positive/ negative curvature of a structure embedded in S. A surface is orientable, when it has two sides, or it is non-orientable, when it has only one side, like the Möbius strip. Curvature (see Diudea and Nagy, 2007) is the amount by which a geometric object deviates from the planarity; it is
usually measured as the *Gaussian curvature K,* $\int_S KdS = 2\pi\chi$ ; a combinatorial curvature was also proposed (Klein and Liu, 1994; Babić *et al*. 2001; Higuchi, 2001; Klein, 2002).

Euler characteristic can be calculated for general surfaces as the alternating sum of figures of dimension/rank (Schulte, 1985, 2014) $k$ :

$$\chi(S) = f_0 - f_1 + f_2 - f_3 + ..., \qquad (4)$$

where $f_0$ is a vertex, $f_1$ is an edge, $f_2$ is a face, $f_3$ is a cell… $f_k$ being a facet of rank $k$; a structure will have the rank k if there are substructures/facets up to the rank $k$-1 and obey relation (4), that in case S=sphere, alternates 2 and 0 for odd and even rank, respectively.

## 2. DESCRIPTORS OF TOPOLOGICAL SYMMETRY

### 2.1 Centrality index

A layer matrix (Diudea, 1994) is built up on a layer partition of a vertex $i$ in the graph $H(V,E)$:
$H(i) = \{H(i)_j, j \in [0, ecc_i] \;\; and \;\; v \in H(i)_j \Leftrightarrow d_{iv} = j\}$

where $ecc_i$ is the eccentricity of $i$ (i.e., the largest distance from $i$ to the other vertices of the graph). The entries in a layer matrix, $LM$, collect the vertex property pv (a topological, chemical, or physical property) for all the vertices $v$ belonging to the layer $H(i)_j$: $[LM]_{ij} = \sum_{v \in G(i)_j} p_v$ located at distance $j$ from vertex $i$. The matrix LM is

defined as: $LM(H) = \{[LM]_{ij};\ i \in V(H);\ j \in [0, d(H)]\}$, where $d(H)$ is the diameter of the graph. The dimensions of the matrix is $n \times (d(H)+1)$; the zero-distance column is just the column of vertex properties. The most simple layer matrix is the vertex counting property. Hereafter, as a property is considered the number of rings R around each vertex while the layer matrix is named LR. Layer matrices are used to derive the indices of centrality C($LM$), that quantify the centrality of vertices (Diudea and Ursu, 2003).

$$c_i(LM) = \left[ \sum_{k=1}^{ecc_i} \left( [LM]_{ik}^{2k} \right)^{1/(ecc_i)^2} \right]^{-1} \qquad (5)$$

2.2 Ring signature index

Ring Signature Index $RSI$ collects the rings around the vertices of a network, and is defined (Diudea, 2016; Nagy and Diudea, 2016) as follows:

$$P(x)_i = \sum_s s \cdot x^{k_s}$$
$$RS_i = P_i`(1) / P_i(1) \qquad (6)$$
$$RSI = (1/qv) \sum_i RS_i$$

In the above, $P(x)_i = \sum_s s \cdot x^{k_s}$ is the polynomial of „ring occurrence" or the „ring signature", or even the „vertex configuration", with $s$ being the size of a „strong" ring occurring $k_s$-times around each point $i$. Next, $RS_i$ calculates a „mean ring signature" as the ratio (in $x$=1) of the first derivative to the „zero" derivative of the ring occurrence polynomial. Finally, the summation of $RS_i$ over all vertices $i$ is again mediated to the number of vertices and to the topological symmetry of the network, by the normalization with the number of vertex equivalence classes.

3. STRUCTURE BUILDING

Design of structures herein studied may be achieved by operations on maps. A map is a combinatorial representation of a (closed) surface, e.g., the polyhedral graphs. Several operations on maps are known and used for various purposes. More about such operations the reader can find in (Pisanski and Randić, 2000; Diudea *et al*. 2006; Diudea and Nagy, 2007; Diudea, 2004, 2005, 2010, 2013).

**Dual** $d$(P) is obtained by putting a point in the center of each face of a polyhedron $P$, next joining two such points if their corresponding faces share a common edge. Vertices of $d$(P) represent faces in the parent polyhedron and *vice-versa.* Dual of the dual returns the original polyhedron: $d(d(P)) = P$. Tetrahedron T is self-dual while the other Platonics (cube C; octahedron O; dodecahedron D and icosahedron I) form dual pairs: $d(C) = O$; $d(D) = I$.

**Medial** $m$(P) can be achieved putting a point in the middle of each parent edge and join two such points if the edges span an angle while the parent vertices are cut off. Medial is a 4-valent graph, symmetric between the parent and its dual, that is $mdM=mM$. The figure type of transformed map is: $\{e, 2e, e+2\}$.The medial operation rotates the parent $s$-gonal faces by $\pi/s$. By medial, edges of the parent polyhedron are reduced to a point; this property can be used in topological analysis of edges. Similarly, the points of the dual give information on the faces of a polyhedron.

**Truncation** $t$(P) is achieved by cutting off the neighborhood of each vertex by a plane close to the vertex, such that it intersects each edge incident in the vertex. The resulted truncated map (i.e., polyhedron) is always a three-connected one. The truncated polyhedron is of the type $\{2e, 3e, e+2\}$,

where *e* denotes the number of edges in the parent object while the numbers within brackets refer, subsequently, to the vertices, edges and faces of the truncated transform.

**Polygonal** $p_k$(P) operation is achieved by adding a new vertex in the center of each face of a polyhedral graph, next put *k*-3 points on the boundary edges. Connect the central point with one vertex on each edge (the endpoints included): the parent face will be covered by triangles (*k*=3), squares (*k*=4) and pentagons (*k*=5), respectively. The transformed polyhedron is of the type: {(*k*-2)*e*+2, *ke*, 2*e*}.

**Snub** is the dual of $p_5$ operation: $s$(P) = $d(p_5$(P) and $s$(P) = $s(d$(P)). The snub polyhedron is of the type: {2*e*, 5*e*, 3*e*+2}. In case P = T, the snub is the icosahedron: $s$(T) = I.

**Operation $s_2$** can be achieved by putting four vertices on each edge of the parent map *M* ($e_4$ operation) and next join these new vertices in order (-1, +3): $s_2 = j_{(-1,+3)}e_4$(P). It insulates the double sized parent faces by pentagons and parent vertices by pentagon *k*-multiples; the transformed objects are non-chiral. The transformed map is of the type: {*v*+4*e*, 7*e*, f+2*e*}. Map operation preserves the symmetry and genus of the parent structure.

### 3.1 Multitori

The building of multitori (Diudea and Petitjean, 2008, Diudea, 2010) herein studied may occur as a self-assembling of monomers; let us start from the cube C and make its snub, $s$(C), by dualizing the $p_5$(C) transform (Figure 4, top); since $p_5$-operation is *prochiral*, all the thansforms involving this map operation will be chiral structures. Suppose the snub cube is realized by atoms of different radius, *e.g.,* one snub cube is made by Carbon atoms and the other by Silicon or Germanium, so that *a* „cage-in-cage" structure is obtained.

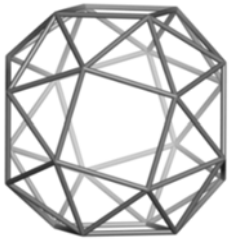

($s$(C)R.24=$d(p_{5\_2}$(C)).24

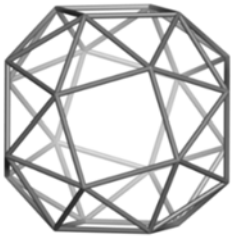

($s$(C)S.24=$d(p_{5\_1}$(C)).24

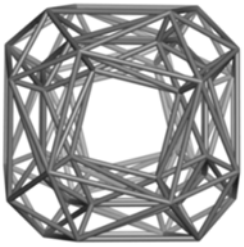

$C_{48}$S=($s$(C)R@$s$(C)R)7S.48

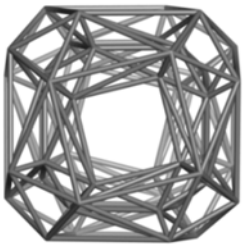

$C_{48}$R=($s$(C)S@$s$(C)S)7R.48

**Figure 4:** Snub cube (top) and its dimer (bottom) as chiral pairs.

A supplementary interaction along the diagonal of quadrilaterals generated on the borders of square parent faces will provide a snub „dimer" (Figure 4, bottom), each vertex/atom having the degree 7; since this diagonal may be drawn to the right or to the left, the number of pair isomers will increase accordingly (see below). Further, the dualization of a 7-connected dimer will provide a multitorus entirely covered by heptagonal faces. Two of such chiral pairs are illustrated in Figure 5: the constitutive name, map operation filiation, symmetry group and order, and the vertex equivalence

classes are included. These structures show the rank 3 or 4, as shown in Table 1 ($P_k/A_k$ = prism/antiprism of $k$-basis).

**Table 1:** Figure count in multitori derived from snub Cube

| Structure | $v$ | $e$ | 3(2) | 4(2) | 7(2) | 2 | 3 | $\chi$ | $g$ | Rank |
|---|---|---|---|---|---|---|---|---|---|---|
| $s$(C) | 24 | 60 | 32 | 6 | 0 | 38 | 0 | 2 | 0 | 3 |
| $C_{112}$ | 112 | 168 | 0 | 0 | 48 | 48 | 0 | -8 | 5 | 3 |
| $d(C_{112})$ | 48 | 168 | 112 | 48 | 0 | 160 | 40 | 0 | 0 | 4 |
| $d(C_{112})$ | | | $A_4$ | $P_3$ | $P_3$* | M | 3 | | | |
| (details for 3) | | | 6 | 8 | 24 | 2 | 40 | | | |

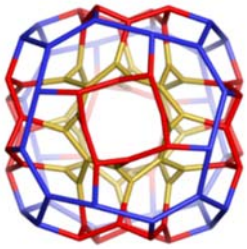

$d$\{($s$(C)R@$s$(C)R)7S.48\}.112
$C_{112}$S=$d$($C_{48}$S).122
S4; ORD 24
Classes: 6: |2{8}; 4{24}|

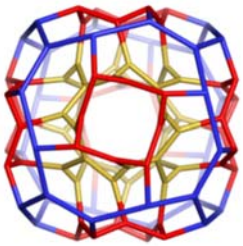

$d$\{($s$(C)S@$s$(C)S)7R.48\}.112
$C_{112}$R=$d$($C_{48}$R).122
S4; ORD 24
Classes: 6: |2{8}; 4{24}|

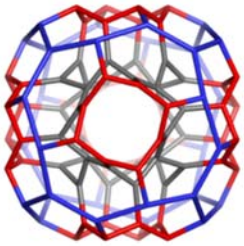

$d$\{($s$(C)R@$s$(C)S)7S.48\}.112
C2 x S4; ORD 48
Classes: 3: |{16}; 2{48}|

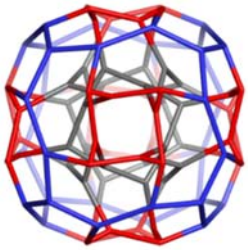

$d$\{($s$(C)R@$s$(C)S)7R.48\}.112
C2 x S4; ORD 48
Classes: 3: |{16}; 2{48}|

**Figure 5:**. Dual of snub cube dimers

Data about the topological symmetry of $C_{112}$ isomers are given in Table A2 (Additional Materials).

### 3.2 Multishell clusters

In the following the construction of three isomers, illuatrated in Figure 6, is detailed.

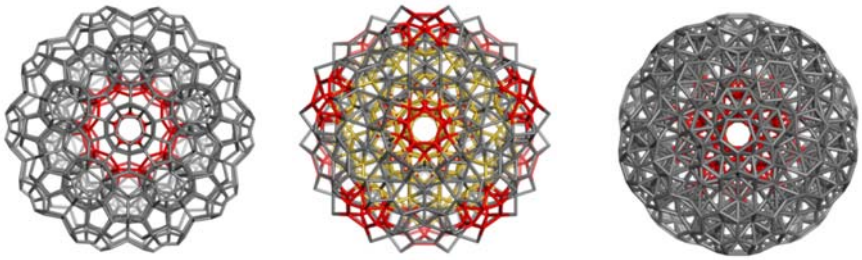

$C_{60}@C_{750}.810$ $C_{130a}@12C_{130a}.810$ $C_{130a}@12C_{13a}.810$

$d(m(C_{45})204).810$ $d(t(C_{45})408).810$

**Figure 6:** Multi-shell clusters of Icosahedral symmetry C2 x A5 and rank higher than 3

The cluster $C_{810} = C_{60}@C_{750}.810$ (*i.e.*, $C_{60}@(12C_{20};20C_{24})@(60C_{20}).810$) of rank 4 (Table 2) was made by gluing $C_{60}$ inside the central hollow of $C_{750}$ (Figure 7); the last one can be designed (Stefu *et al*. 2015; Diudea 2016) by the following sequence of operations: $t_{sel}(p_4(C_{60})).330$; $s_2(C_{60}).420$; $t_{sel}\{p_4(C_{60}))@s_2(C_{60})420\}.750$; the symbol $t_{sel}$ means the truncation of only selected vertices. Structure $C_{750} = C_{60}Y(60C_{20}).750$ is a "spongy" one, with the central hollow of exact topology of $t_{sel}(p_4(C_{60})).330$. Letter Y indicates that $C_{750}$ is a "hyper-$C_{60}$", with the main topology of $C_{60}(I_h)$; in this case, any atom/vertex in $C_{60}$ is formally changed by a $C_{20}$ cell.

**Table 2:** Figure count for $C_{810}$ and its precursor.

| Structure | v | e | 5(2) | 6(2) | 2 | $C_{20}$ | $C_{24}$ | M | 3 | χ | Rank |
|---|---|---|---|---|---|---|---|---|---|---|---|
| $C_{750}$ | 750 | 1350 | 642 | 20 | 662 | 60 | 0 | 2 | 62 | 0 | 4 |
| $C_{810}$ | 810 | 1500 | 744 | 40 | 784 | 72 | 20 | 2 | 94 | 0 | 4 |

Let now truncate the dual of $C_{750}$, namely $d(C_{750}).630$ cluster; the resulted structure, $t(d(C_{750}).630).3600$ (Figure 8), is a hyper-$C_{60}$ one, $C_{60}Y(60C_{60}; 90P_5).3600$, with a whole $C_{60}$ cluster instead of each vertex/atom in the parent $C_{60}$; the $C_{60}$-units are joined by pentagonal prisms $P_5$. The cluster $C_{3600}$ is a spongy-one, of rank 4 (Table 3), in other words, it is a multitorus embedded in a surface of genus 16 ($\chi = -30$) (a similar structure was reported by Bhattacharya et al. 2016).

**Table 3:** Figure count for $C_{3600}$ and its precursor.

| Structure | v | e | 3(2) | 4(2) | 5(2) | 6(2) | 2 | U | Py4 | P5 | P6 | M | 3 | χ | g | Rank |
|---|---|---|---|---|---|---|---|---|---|---|---|---|---|---|---|---|
| d(C750) | 630 | 2250 | 1650 | 450 | 24 | 40 | 2164 | 60 | 450 | 12 | 20 | 2 | 544 | 0 | 0 | 4 |
| t(d(C750)) | 3600 | 5850 | 0 | 450 | 720 | 1200 | 2370 | 60 | 0 | 90 | 0 | 0 | 150 | -30 | 16 | 4 |

Note that any cluster may be decomposed in several ways, some key-substructures being illustrated at the bottom of figures; accordingly, several names are used for a same structure, with the aim of a better detailing its composition. However, the fragment union (i.e., re-construction) finally will provide a single structure, the figures/substructures of which are counted to find its rank. Here, rank (Schulte, 1985, 2014) is preferred to the term "(space) dimension" since our description in a topological one, thus the geometric aspects (angles and bond length) are disregarded.

Data about the topological symmetry of $C_{750}$ and related structures are listed in Table A2 (Additional Material).

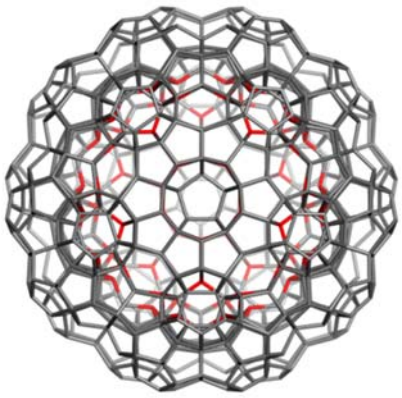

$C_{750}=C_{60}Y(60C_{20}).750$
$t_{sel}\{P4(C_{60}))@S2(C_{60})420\}.750$

C2 x A5; Classes: 12: |10{60}; {120}; {30}|

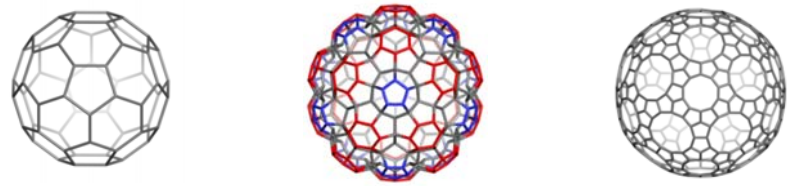

$C_{60}$ $t_{sel}\{P_4(C_{60})\}.330$ $S_2(C_{60}).420$

**Figure 7:** A multi-shell cluster on 750 vertices

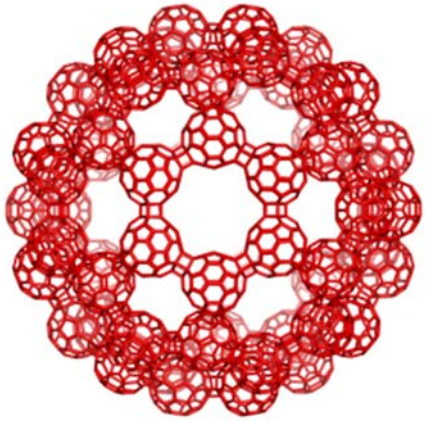

$C_{3600}$
$C_{60}Y(60C_{60}\_P_5).3600$
$C_{60}Y(60C_{60}; 90P_5).3600$
$t(d(C_{750}).630).3600$
C2 x A5; Classes: 32: |28{120}; 4{60}|

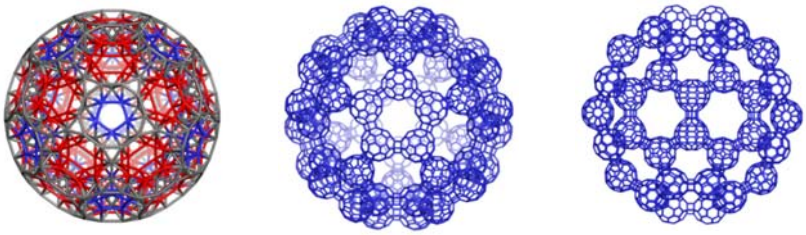

$d(C_{750}).630$ $C_{3600}$ (5) $C_{3600}$ (2)

**Figure 8:** $C_{3600}$ = Truncated dual of $C_{750}$

The two other clusters on 810 atoms in Figure 6 (middle and right) are derived from the Bergman cluster (Bergman et al. 1952; Duneau and Gratias, 2002) $C_{45}$ (Figure 9), a cluster of rank 5 (Table 4).

Table 4. Figure count in $C_{45}$ and IP structures

| Structure | v | e | 3(2) | 2 | T(3) | U(3) | 3 | 4 | χ | Rank |
|---|---|---|---|---|---|---|---|---|---|---|
| $C_{45}$ | 45 | 204 | 290 | 290 | 130 | 12 | 142 | 13 | 2 | 5 |
| IP | 13 | 42 | 50 | 50 | 20 | 1 | 21 | 0 | 0 | 4 |

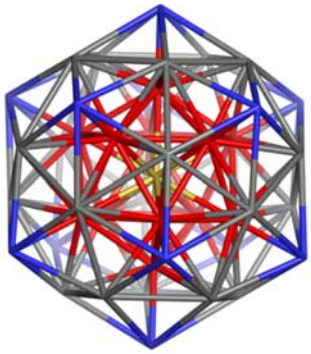

$C_{45}$
IP@12IP.45
($P^{12}$@I)@*st*(D)).45
(IP)Y(12IP).45
20T@(20T;30T)@60T.45
C2 x A5; Classes: 4: |2{12}; {20}; {1}|

$P^{12}$@I.13=IP.13

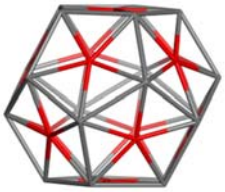

*st*(D).32

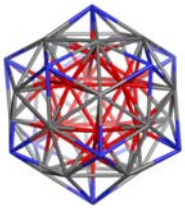

I@*st*(D).44

**Figure 9:** $C_{45}$ = Bergman cluster (details)

The medial of $C_{45}$, *i.e.* the cluster $C_{204}$=*m*($C_{45}$) (Figure 10) transforms by dualization (*d*(*m*($C_{45}$)204).810) into $C_{130a}$@12$C_{130a}$.810 (Figure 3, middle), a cluster of rank 4 (Table 5).

Table 5. Figure count in *d*($C_{204}$).810 (Rank 4) and related structures

| Struct. | *v* | *e* | 2(3) | 2(4) | 2(5) | 2 | 3(D;I) | 3(C) | 3($Py_5$) | 3(*m*$P_5$) | 3(O) | M | 3 | χ |
|---|---|---|---|---|---|---|---|---|---|---|---|---|---|---|
| | 81 | 225 | | | | 169 | | | | | | | 25 | |
| 810 | 0 | 0 | 690 | 780 | 228 | 8 | 13 | 130 | 0 | 114 | 0 | 1 | 8 | 0 |
| | 13 | | | | | | | | | | | | | |
| $130_a$ | 0 | 330 | 90 | 120 | 24 | 234 | 1 | 20 | 0 | 12 | 0 | 1 | 34 | 0 |
| | 20 | | | | | | | | | | | | 14 | |
| 204 | 4 | 870 | 810 | 0 | 12 | 822 | 1 | 0 | 12 | 0 | 130 | 1 | 4 | 0 |
| *m*(I) | 42 | 150 | 130 | 0 | 12 | 142 | 1 | 0 | 12 | 0 | 20 | 1 | 34 | 0 |

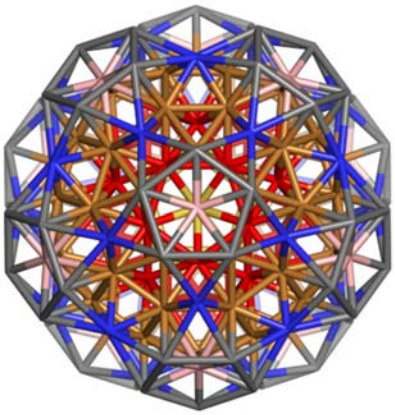

$m(C_{45})$.204
$C_{42}$@12$C_{42}$.204
I@(12I;20×(2O))@(30O;12(P@5O)16).204
C2 x A5; Classes: 6: |2{60}; 2{12}; 2{30}|

I@ID.42=$C_{42}$
M(IP).42

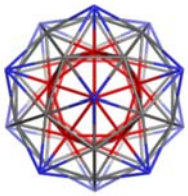

$C_{45}$
IP@12IP.45

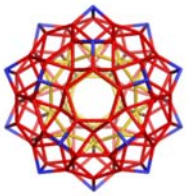

$C_{130a}$=D($C_{42}$).130
$C_{20}$@(12(M($P_5$));20C).130

**Figure 10:** $C_{204}$ = medial of Bergman cluster

Data about the topological symmetry of $C_{750}$ and related structures are listed in Table A3 (Additional Material).

The truncated $C_{45}$, *i.e.* the cluster $C_{408}$=*t*($C_{45}$) (Figure 11) transforms by dualization *d*(*t*($C_{45}$)408).810 into $C_{130b}$@12$C_{130b}$.810 (Figure 3, right), a cluster of rank 6 (Table 6). In addition, Table A4 (Additional Material) provides data about its topological symmetry.

Details within the amazing structure $C_{130b}$@12$C_{130b}$.810 are shown in Figure 12; there are interlaced $C_{230}$=ID@12ID.230 (with all degree 12 vertices, when is "endo" $C_{230}$@$C_{810}$) and 13 $C_{20}$ cells disjoint to each other (inside the $C_{810}$ hull, as shown in the left-bottom corner of Figure 12). Note that $C_{230}$=*m*($C_{20}$)@12*m*($C_{20}$).230 can be designed from $C_{20}$@12$C_{20}$.130 by the medial operation. Data about the symmetry of $C_{230}$ (free or "immersed" within $C_{810}$) are provided in Figure 12 and in Table A5 (Additional Material).

Table 6. Figure count in *d*($C_{408}$).810 and related structures (Rank 4 to 6).

| *v* | *e* | 2(3) | 2(5) | 2(6) | 2 | 3(T/TT) | U | 3($A_5$) | 3($Py_k$) | M | 3 | 4 | 5 | 6 |
|---|---|---|---|---|---|---|---|---|---|---|---|---|---|---|
| 810 | 3030 | 2770 | 342 | 120 | 3232 | 650 | 13 | 228 | 120 | 1 | 1012 | 13 | 13 | 0 |
| $130_b$ | 450 | 410 | 36 | 30 | 476 | 100 | 1 | 24 | 30 | 1 | 156 | 2 | 2 | - |
| 110 | 360 | 320 | 24 | 30 | 374 | 80 | 1 | 12 | 30 | 1 | 124 | 0 | - | - |

| | | | | | | | | | | | | | | |
|---|---|---|---|---|---|---|---|---|---|---|---|---|---|---|
| 50 | 150 | 110 | 24 | 0 | 134 | 20 | 1 | 12 | 0 | 1 | 34 | 0 | - | - |
| 408 | 1074 | 520 | 12 | 290 | 822 | 130 | 12 | 12 | 12 | 1 | 167 | 13 | 2 | - |
| 84 | 192 | 80 | 12 | 50 | 142 | 20 | 1 | 0 | 12 | 1 | 34 | 0 | - | - |

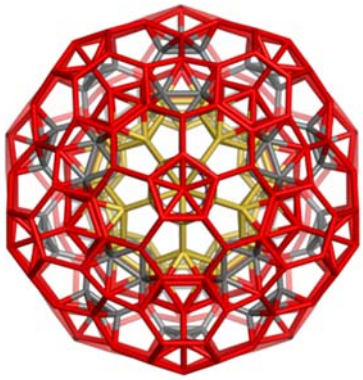

*t*($C_{45}$).408
$C_{84}$@12$C_{84}$.408
(I@20×2TT)@(12I;30TT)@12($Py_5$@5TT)@$C_{180}$.408
C2 X A5; Classes: 10: |6{60}; 4{12}|

*t*(IP).84=$C_{84}$

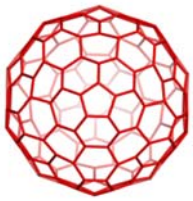

$C_{180}$($I_h$)

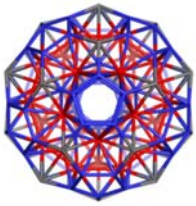

$C_{130b}$
*d*($C_{84}$).130
$C_{50}$@$C_{110}$.130

**Figure 11:** $C_{408}$ = Truncated $C_{45}$ cluster

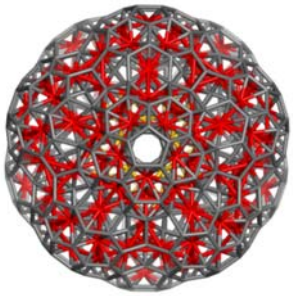

$C_{230}$@$C_{810}$_d($C_{408}$)
C2 X A5; ORD=120
Classes: 15: |10{60}; {120}; 3{20}; {30}|

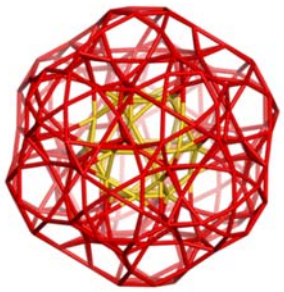

$C_{230}$ = ID@12ID
C2 X A5; ORD=120
Classes: 5: |{30}; {20}; 3{60}|

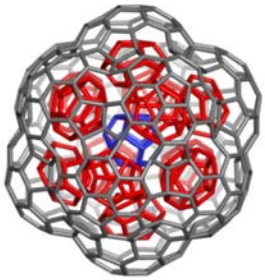

Complement ($C_{810}$-$C_{230}$).580
(13 $C_{20}$, disjoint)

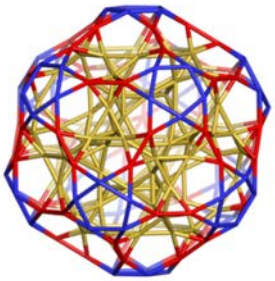

$C_{230}$
(ID@12half(ID))@tD.110
(yellow)

**Figure 12**: Inside $C_{810}$_d($C_{408}$) = $C_{130b}$@12$C_{130b}$.810

Note that, with the Y-symbol for a hyper-structure, the name of the above clusters, and IP being the centered Icosahedron $P^{12}$@I.13 ($P^{12}$ meaning the central point connected to the 12 points of Icosahedron) can be written: (IP)Y(12IP).45; (IP)Y(12$C_{130a}$).810; (IP)Y(12$C_{130b}$).810; (IP)Y(12$C_{42}$).204 and (IP)Y(12$C_{84}$).408. From the above data, it is clear that all these clusters preserve the Icosahedral symmetry (i.e., C2 × A5; ORD 120) of the parent IP cluster (itself of rank 4). Also note that IP is the cell-dual of D@12D.130. (C2 × A5; Classes: 4: |2{20}; {30}; {60}|) .In the derived clusters above listed, the 12 units intersect to each other while a 13th one appears in the centre of structure (to be counted, or not – see M = 1 in Tables 5 and 6).

## 4. TOPOLOGICAL SYMMETRY OF COMPLEX CLUSTERS

Multitori are graphs embedded in surfaces of high genera (Diudea and Nagy, 2007; Diudea and Petitjean, 2008). Tables 1 and 3 show negative values for Euler characteristic ($\chi$ = -8; $g$= 5 and $\chi$ = -30; $g$ = 16) for $C_{112}$ and $C_{3600}$, respectively, meaning the embedding surfaces have negative curvatures. Accordingly, $C_{112}$ is of rank 3 while $C_{3600}$ of rank 4, meaning the two characteristics: genus and rank (both of them contributing to the structure complexity) do not exclude, on the contrary, join to build the beauty of a structure. Majority of the herein studied structures have ranks between 4 and 6 (see Tables 1 to 6). In addition, the multitori $C_{112}$ are chiral, a molecular property.

Searching for the atom classes by face/ring count provides the „chemical atom type" if the rings around each atom (counted by RSI – Eq. 6) are „strong rings" („strong" denoting a ring that is not the sum of other smaller rings – Blatov *et al*. 2010); however, by enlarging the rings to „circuits" of various length (the upper bound involves the counting of circuits of length 2$d$+1, $d$ being the diameter of the graph), then different, topologically distinct, vertex classes are revealed (finally correctly discriminating all the classes of a graph, as given by performing the permutations within the adjacency matrix, a much more time-consuming procedure). If the „ring signature" is collected in a layer matrix (Diudea, 1994; Diudea and Ursu, 2003), the centrality index calculated on it, cf. Eq. 5, will distinguis all these distinct vertices, at the early level of strong rings (see Tables A1 to A5). The same vertex classes are obtained with the layer matrix of topological distances, an even faster procedure, compared to the ring counting. An example of topological symmetry calculation is given in Table 7 (while for the other herein discussed structures data are given in Additional Materials.

Table 7. Topological symmetry by ring count (cf. Eqs. 6) and centrality C-index (cf. Eq. 5) (in decreasing order of centrality) in $C_{810}$_d($C_{408}$) and its relatives.

| | Structure (RSI) | $R_{min}$ | $R_{max}$ | Deg | Signature ($C_{min}$; $C_{max}$) | Classes {elements} |
|---|---|---|---|---|---|---|
| 2 | $C_{84}$ | 3 | 6 | 6 | 3^5.5^5.6^25 | **3**: {12}; |
| | (1.377551) | | | 6 | 3^5.6^5 | {12}; |
| | | | | 4 | 3^2.5.6^3 | {60} |
| | LM($C_{84}$) | 3 | 6 | 6 | (0.149447) | **3**: {12}; |
| | | | | 6 | (0.118464) | {12}; |
| | | | | 4 | (0.097012) | {60} |
| 4 | $C_{408}$ | 3 | 6 | 6 | 3^5.5^5.6^25 | **6**: {156}; |
| | (1.246499) | | | 6 | 3^5.5^2.6^6 | {60}; |
| | | | | 5 | 3^3.5^2.6^8 | {60}; |
| | | | | 6 | 3^5.6^5 | {12}; |
| | | | | 4 | 3^2.5.6^6 | {60}; |
| | | | | 4 | 3^2.5.6^3 | {60} |
| | LM($C_{408}$) | 3 | 6 | 4; 5; 6 | (0.095120) | **10**:4×{12}; |
| | | | | | (0.057074) | 6×{60} |
| 5 | $C_{810}$ = d($C_{408}$) | 3 | 6 | 12 | 3^21.5^3.6^60 | **7**: {110}; |
| | (8.116238) | | | 12 | 3^21.5^2.6^41 | {60}; |
| | | | | 12 | 3^21.5^2.6^40 | {60}; |
| | | | | 6 | 3^6.5^3.6^33 | {280}; |
| | | | | 6 | 3^6.5^2.6^24 | {60}; |
| | | | | 6 | 3^9.6^3 | {60}; |
| | | | | 5 | 3^5.5.6^13 | {180} |
| | LM($C_{810}$) | 3 | 6 | (5;6;12) | (0.104546) | **15**: 3×{20}; |
| | | | | | (0.065660) | {30};10×{60} |
| | | | | | | {120} |

These theoretical tools, implemented in the Nano Studio software (Nagy and Diudea, 2009) enable the study the topological symmetry of rather complex structures. The structures were designed by CVNET software (Stefu and Diudea, 2005), the both programs being developed at TOPO GROUP, „Babes-Bolyai" University, Cluj, Romania. The classes found by C-index were confirmed by permutations on the corresponding adjacency matrix, performed by Mathematica and GAP software (Groups, Algorithms and Programming, http://www.gap-system.org.).

## 5. CONCLUSIONS

Topological symmetry may be calculated either by permutations on the adjacency matrix of its associate graph or by calculating the equivalence classes of substructures by some topological indices. In this paper, the vertex equivalence classes of some high rank and high genus clusters, with icosahedral and octahedral symmetry, were obtained by using two topological indices: ring signature index RSI and centrality index C; these parameters were computed, by the original Nano Studio software, both in isolated structures or in selections "immersed" on the bulk networks and the results were confirmed by permutation calculations, performed by the GAP software. Design of high rank

and genus multi-shell clusters was performed at TOPO GROUP CLUJ by the original CVNET and Nano Studio software programs.

**Acknowledgement**. The authors are endebted to Dr. Csaba Nagy, Faculty of Chemistry and Chemical Engineering, „Babes-Bolyai" University, Cluj, Romania, for computer assistance.

## REFERENCES

Ashrafi, A.R., Kooperazan-Moftakhar, F., Diudea, and M.V., Stefu, M. (2013) Mathematics of D5 Network. In: Diudea, M.V. and Nagy, C.L. (Eds) *Diamond and Related Nanostructures*, Springer, Dordrecht Heidelberg New York London, p 321-333.

Babić, D., Klein, D.J., and Schmalz, T.G. (2001) Curvature matching and strain relief in bucky-tori: usage of $sp^3$-hybridization and nonhexagonal rings*, Journal of Molecular Graphics & Modelling*, 19, 223-231.

Bergman, G., Waugh, J. L. T. & Pauling, L. (1952) Crystal structure of the intermetallic compound Mg32(Al, Zn)49 and related phases, *Nature*, 169, 1057-1058.

Bhattacharya, D., Klein, D.J. and Ortiz, Y. (2016) The astounding buckyball buckyball, *Chemical Physics Letters*, 647, 185-188.

Blatov, V.A., O'Keeffe, M. and Proserpio, D.M. (2010) Vertex-, face-, point-, Schläfli-, and Delaney-symbols in nets, polyhedra and tilings: recommended terminology, *CrystEngComm*. 12, 44–48.

Diudea, M.V. (1994) Layer Matrices in Molecular Graphs. *Journal of Chemical Information and Computer Sciences*, 34, 1064-1071.

Diudea, M.V. (2004) Covering forms in nanostructures. *Forma* (Tokyo), 19, 131–163.

Diudea, M.V. (2005) Nanoporous carbon allotropes by septupling map operations. *Journal of Chemical Information and Modeling*, 45, 1002–1009.

Diudea, M.V. (2010) *Nanomolecules and Nanostructures – Polynomials and Indices*, MCM, No 10, Univ Kragujevac, Serbia.

Diudea, M.V. (2013) Quasicrystals, between spongy and full space filling. In: Diudea, M.V. and Nagy, C.L. (eds) *Diamond and Related Nanostructures*. Springer, Dordrecht Heidelberg New York London, p 333-383.

Diudea, M.V. (2016) Multi-shell polyhedral clusters, Springer (in preparation).

Diudea, M.V. and Nagy, C.L. (2007). *Periodic Nanostructures.* Springer, Dordrecht.

Diudea, M.V. and Nagy, CL (Eds) (2013). *Diamond and Related Nanostructures*, Springer, Dordrecht Heidelberg New York London.

Diudea, M.V. and Petitjean, M. (2008) Symmetry in Multi-tori. *Symmetry: Culture and Science*, 19, no. 4, 285–305.

Diudea, M.V. and Ursu, O. (2003) Layer matrices and distance property descriptors. *Indian Journal of Chemistry, A,* 42, no. 6, 1283-1294.

Diudea, M.V., Stefu, M., John, P.E., and Graovac, A. (2006) Generalized operations on maps. *Croatica Chemica Acta*, 79, 355-362.

Duneau, M. and Gratias, D. (2002) Covering Clusters in Icosahedral Quasicrystals. In: Coverings of Discrete Quasiperiodic Sets. Vol. 180 of the series Springer Tracts in Modern Physics, pp. 23-62.

Euler, L (1752-3) Elementa doctrinae solidorum-Demonstratio nonnullarum insignium proprietatum, quibus solida hedris planis inclusa sunt praedita*, Novi Comment Acad. Sc. Imp. Petropol.,* 4, 109-160.

GAP - Groups, Algorithms, Programming - a System for Computational Discrete Algebra, **GAP 4.7.5** release, (2014); **http://www.gap-system.org**

Harary, F. (1969) *Graph Theory*. Addison–Wesley, Reading, MA.

Higuchi, Y. (2001) Combinatorial curvature for planar graphs, *Journal of Graph Theory,* 38, 220–229.

Hungerford, T. W. *Algebra*. Reprint of the 1974 original. Graduate Texts in Mathematics, 73. Springer–Verlag, New York–Berlin, 1980.

Klein, D.J. (2002) Topo-combinatoric categorization of quasi-local graphitic defects*, Physical Chemistry and Chemical Physics,* 4, 2099–2110.

Klein, D.J. and Liu, X. (1994) Elemental Carbon Isomerism, *International Journal of Quantum Chemistry*, S, 28, 501-523.

Nagy, C.L. and Diudea, M.V. (2009) NANO–Studio software, Babes–Bolyai Univ., Cluj.

Nagy, C.L. and Diudea, M.V. (2016) Ring Signature Index. MATCH Communications in Mathematical and Computational Chemistry (accepted).

Pisanski, T. and Randić, M. (2000) Bridges between geometry and graph theory. *Geometry at Work*. *MAA Notes*, 53, 174–194.

Schulte E. (1985) Regular incidence-polytopes with Euclidean or toroidal faces and vertex-figures. *Journal of Combinatorial Theory, A*, 40, no. 2, 305-330.

Schulte E (2014) Polyhedra, complexes, nets and symmetry. *Acta Crystallographica, A,* 70, 203-216

Stefu, M. and Diudea, M.V. (2005) CageVersatile_CVNET software, Babes–Bolyai Univ, Cluj.

Stefu, M.. Parvan-Moldovan, A. Kooperazan-Moftakhar, F. and Diudea, M.V. (2015) Topological symmetry of $C_{60}$-related multi-shell clusters. *MATCH Communications in Mathematical and Computational Chemistry, 74, 273-284*